

Some new observations for the Georgi-Machacek scenario with triplet Higgs scalars

Rituparna Ghosh^{✉*} and Biswarup Mukhopadhyaya[†]

Department of Physical Sciences, Indian Institute of Science Education and Research, Kolkata, Mohanpur - 741246, India



(Received 5 January 2023; accepted 31 January 2023; published 27 February 2023)

The Georgi-Machacek model, introducing a complex and a real scalar triplet as additional components of the electroweak symmetry breaking sector, enables substantial triplet contributions to the weak gauge boson masses, subject to the equality of the complex and the real triplet vacuum expectation values (vev) via a custodial SU(2) symmetry. We present an updated set of constraints on this scenario, from collider data (including those from $137/139 \text{ fb}^{-1}$ of luminosity at the Large Hadron Collider), available data on the 125 GeV scalar, indirect limits, and also theoretical restrictions from vacuum stability and unitarity. It is found that some bounds get relaxed, and the phenomenological potential of the scenario is more diverse, if the doubly charged scalar in the spectrum can decay not only into two like-sign W 's but also into one or two singly charged scalars. Other interesting features are noticed in a general approach, such as substantial $\gamma\gamma$ and $Z\gamma$ branching ratios of the additional custodial singlet scalar and appreciable strength of the trilinear interaction of a charged scalar, the W and the Z . Finally, we take into account the possibility of custodial SU(2) breaking, resulting in inequality of the real and the complex scalar vevs which, too, in principle may allow large triplet contribution to weak boson masses. Illustrative numerical results on the modified limits and predictions are presented, once more taking into account all the constraints mentioned above.

DOI: [10.1103/PhysRevD.107.035031](https://doi.org/10.1103/PhysRevD.107.035031)

I. INTRODUCTION

As the electroweak symmetry breaking sector continues to be closely scrutinized both theoretically and experimentally, a query persists far and wide. It is as follows: can the vacuum expectation values (vev) of other scalars, not necessarily $SU(2)_L$ doublets, also contribute substantially to the W - and Z -boson masses, besides the 125 GeV particle that arises overwhelmingly out of a doublet [1]? SU(2) triplet scalars are especially interesting in this connection, since a) they may occur in some Grand Unified Theories [2,3] as well as in left-right symmetric scenarios [4–7] and b) they offer a mechanism for generating Majorana masses for left-handed neutrinos, called the Type-II seesaw mechanism [8,9]. However, there is a strong constraint on, say, a single $Y = 2$ complex triplet vev from the ρ parameter [6,10], whose tree-level value is given by $\rho = \frac{m_W^2}{m_Z^2 \cos^2 \theta_W} = 1$, where θ_W is the weak boson mixing angle. The vev of a

stand-alone triplet thus cannot exceed about 4 GeV; hence, its contribution to the weak boson masses is rather meager. A frequently discussed model in this context is the one proposed first by Georgi and Machacek (GM), where one complex triplet (χ , $Y = 2$) and one real triplet (ξ , $Y = 0$) were introduced in addition to the doublet Φ of the standard model (SM) [11,12]. Such a model can be associated with “composite Higgs” scenarios [13], but it is of sufficient interest on its own. It ensures $\rho = 1$ at tree level if the two triplets have equal vev, ensured with the help of a global SU(2) as custodial symmetry [14].¹ Thus, in the simplest case, one has $v_\chi = v_\xi$. In this case, $s_H = \frac{2\sqrt{2}v_\chi}{\sqrt{v_\Phi^2 + 8v_\chi^2}}$ emerges as a measure of the triplet contribution to the gauge boson masses. Attempts have been made in recent works to obtain upper bounds on this important parameter from experimental as well as theoretical considerations, mostly as functions of the mass of the doubly charged component of the triplet χ , which is one distinct ingredient of this scenario. The available limits used data from the LHC as well as indirect limits such as those from rare decay processes as also precision electroweak measurements.

*rg20rs072@iiserkol.ac.in

†biswarup@iiserkol.ac.in

Published by the American Physical Society under the terms of the Creative Commons Attribution 4.0 International license. Further distribution of this work must maintain attribution to the author(s) and the published article's title, journal citation, and DOI. Funded by SCOAP³.

¹Studies on variants of the model including additional symmetries are also found in the literature, but we are not restricting ourselves by such considerations here [15].

In this work, we generalize and update these limits, which enable one to extend the region of the GM parameter space that can be constrained, and also include additional possibilities in the particle spectrum of this kind of a theory. In particular, the new features of our analysis are as follows:

- (1) Available updated limits from the LHC data have been incorporated. Most important of these are the new limits on doubly charged scalar production via vector boson fusion (VBF) [16] and also Drell-Yan (DY) [17] processes. The latter is particularly important because it predicts production cross sections which are four times as much as those for singly charged scalars.
- (2) The previous search limits were obtained using the assumption that the doubly charged scalar decays exclusively into two same-sign W bosons [18–20]. This restricted the analyses to a small region of the parameter space. We, on the other hand, included possibilities where the doubly charged state can also decay into a singly charged state and a W , as also into two singly charged states. We find that some such cases allow higher triplet contributions to the weak boson masses than come with the same-sign W -pair decay alone.
- (3) We have included the possibility of $v_\chi \neq v_\xi$, i.e., of broken custodial $SU(2)$. The consequent shift in parameter values in the scalar potential is not fully calculable unless one knows the UV completion of the theory, which has to be at relatively low scales if the triplet-dominated states have to make any difference to phenomenology [21–23]. Using some phenomenological limits on the parameter shift, we have computed the changes in contributions to the rates of various collider phenomena and obtained modified limits on the “effective” triplet vev for various masses of the doubly charged states, again allowing for single-channel as well as two- and three-channel decays of the latter.

- (4) One characteristic feature of such scenarios is the existence of nonvanishing trilinear interactions involving a charged scalar, a W and a Z , something that is not permissible with scalar doublets alone [24]. Such interactions, essentially related to the triplet vev value, bring in additional collider phenomenology [6,25–29]. We have indicated the upper limits on the strength of such interactions, for both $v_\chi = v_\xi$ and $v_\chi \neq v_\xi$.
- (5) In addition to various experimental limits, direct as well as indirect, we have also included the theoretical limits (arising mostly from unitarity and occasionally from vacuum stability) on the triplet vev, for both $v_\chi = v_\xi$ and $v_\chi \neq v_\xi$. The limits are found to be stronger for high values of the doubly charged scalar mass.
- (6) We have calculated the coupling strength of a neutral scalar that is singlet under custodial $SU(2)$ in this scenario to WW/ZZ [30,31] and $f\bar{f}$, using as reference the corresponding interaction strengths of the SM-like scalar. The $\gamma\gamma$ and $Z\gamma$ [32,33] branching ratios predicted for the same scalar have also been calculated and scanned over the parameter space. This can serve as indicators of the phenomenological potential of this neutral spin-0 state, for instance, the high-luminosity LHC.

We present a brief outline of the GM scenario in Sec. II. Sections III and IV are devoted to the experimental and theoretical limits and some related features of scenarios with $v_\chi = v_\xi$ and $v_\chi \neq v_\xi$, respectively. We summarize and conclude in Sec. V.

II. BRIEF SUMMARY OF THE SCENARIO

The scalar sector of the Georgi-Machacek model [11,12] consists of a $Y = 2$ complex triplet $\chi = (\chi^{++}, \chi^+, \chi^0)$ and a $Y = 0$ real triplet $\xi = (\xi^+, \xi^0, \xi^-)$ along with the usual Standard model doublet. The most general potential preserving a global $SU(2)_L \times SU(2)_R$ is given by [18,19,34]

$$V = \frac{\mu_2^2}{2} \text{Tr}(\Phi^\dagger \Phi) + \frac{\mu_3^2}{2} \text{Tr}(X^\dagger X) + \lambda_1 [\text{Tr}(\Phi^\dagger \Phi)]^2 + \lambda_2 \text{Tr}(\Phi^\dagger \Phi) \text{Tr}(X^\dagger X) + \lambda_3 \text{Tr}(X^\dagger X X^\dagger X) + \lambda_4 [\text{Tr}(X^\dagger X)]^2 - \lambda_5 \text{Tr}(\Phi^\dagger \tau^a \Phi \tau^b) \text{Tr}(X^\dagger t^a X t^b) - M_1 \text{Tr}(\Phi^\dagger \tau^a \Phi \tau^b) (UXU^\dagger)_{ab} - M_2 \text{Tr}(X^\dagger t^a X t^b) (UXU^\dagger)_{ab}, \quad (1)$$

where

$$\Phi = \begin{pmatrix} \phi^{0*} & \phi^+ \\ \phi^- & \phi^0 \end{pmatrix} \quad X = \begin{pmatrix} \chi^{0*} & \xi^+ & \chi^{++} \\ \chi^- & \xi^0 & \chi^+ \\ \chi^{--} & \xi^- & \chi^0 \end{pmatrix} \quad (2)$$

$$U = \begin{pmatrix} -\frac{1}{\sqrt{2}} & 0 & \frac{1}{\sqrt{2}} \\ -\frac{i}{\sqrt{2}} & 0 & -\frac{i}{\sqrt{2}} \\ 0 & 1 & 0 \end{pmatrix}.$$

τ^a s and t^a s are the 2×2 and 3×3 $SU(2)$ generators, respectively.

With this potential, the tadpole conditions always have a solution at $v_\chi = v_\xi$. The $SU(2)_L$ and the $U(1)$ subgroup of $SU(2)_R$ are gauged, and they break down to $U(1)_{\text{EM}}$ via the Higgs mechanism [35,36]. After electroweak symmetry breaking, the vacuum is invariant under the diagonal subgroup of $SU(2)_L \times SU(2)_R$ which is called the custodial $SU(2)$ and ensures $\rho = 1$ at the tree level. At $v_\chi = v_\xi$, $v_\phi^2 + 8v_\chi^2 = v^2 = (246.22 \text{ GeV})^2$. The tadpole conditions

that determine the doublet and the triplet vev in terms of parameters in the potential are given by [18,19]

$$\mu_2^2 + 4\lambda_1 v_\phi^2 + 3(2\lambda_2 - \lambda_5)v_\chi^2 - \frac{3}{2}M_1 v_\chi = 0 \quad (3)$$

$$3\mu_3^2 v_\chi + 3(2\lambda_2 - \lambda_5)v_\phi^2 v_\chi + 12(\lambda_3 + 3\lambda_4)v_\chi^3 - \frac{3}{4}M_1 v_\phi^2 - 18M_2 v_\chi^2 = 0. \quad (4)$$

Since the potential retains a custodial SU(2) after electroweak symmetry breaking (EWSB), the physical states will belong to the irreducible representation of this group. Hence, particles belonging to a particular multiplet will be degenerate in mass. Here, one has a 5-plet, two 3-plet, and two singlet states. One of the 3-plets contains the Goldstone modes that become the longitudinal components of the weak gauge bosons. The 5-plet states are given by

$$H_5^{++} = \chi^{++}, \quad H_5^+ = \frac{\chi^+ - \xi^+}{\sqrt{2}}$$

and a CP -even neutral scalar,

$$H_5^0 = \sqrt{\frac{2}{3}}\xi^0 - \sqrt{\frac{1}{3}}\chi^{0,r}.$$

The physical 3-plet consists of

$$H_3^+ = -s_H \phi^+ + c_H \frac{\chi^+ + \xi^+}{\sqrt{2}}$$

and a CP -odd neutral scalar,

$$H_3^0 = -s_H \phi^{0,i} + c_H \chi^{0,i},$$

where

$$s_H = \frac{2\sqrt{2}v_\chi}{v} \quad \text{and} \quad c_H = \frac{v_\phi}{v}.$$

The masses of these 5-plet and 3-plet scalars are

$$m_{H_5^{\pm\pm}}^2 = m_{H_5^\pm}^2 = m_{H_5^0}^2 = m_5^2 = \frac{M_1}{4v_\chi} v_\phi^2 + 12M_2 v_\chi + \frac{3}{2}\lambda_5 v_\phi^2 + 8\lambda_3 v_\chi^2 \quad (5)$$

$$m_{H_3^\pm}^2 = m_{H_3^0}^2 = m_3^2 = \left(\frac{M_1}{4v_\chi} + \frac{\lambda_5}{2} \right) v^2. \quad (6)$$

The singlet states are given by

$$H^0 = \phi^{0,r}, \quad H^{0r} = \sqrt{\frac{1}{3}}\xi^0 + \sqrt{\frac{2}{3}}\chi^{0,r}.$$

The physical states are combinations of these two and given by

$$h = \cos \alpha \phi^{0,r} - \sin \alpha H^{0r}, \quad H = \sin \alpha \phi^{0,r} + \cos \alpha H^{0r}.$$

The angle α depends on the 2×2 CP -even custodial-singlet scalar mass matrix. The elements of the mass matrix are

$$\mathcal{M}_{11}^2 = 8\lambda_1 v_\phi^2 \quad (7)$$

$$\mathcal{M}_{12}^2 = \frac{\sqrt{3}}{2} v_\phi [-M_1 + 4(2\lambda_2 - \lambda_5)v_\chi] \quad (8)$$

$$\mathcal{M}_{22}^2 = \frac{M_1 v_\phi^2}{4v_\chi} - 6M_2 v_\chi + 8(\lambda_3 + 3\lambda_4)v_\chi^2 \quad (9)$$

$$\tan 2\alpha = \frac{2\mathcal{M}_{12}^2}{\mathcal{M}_{22}^2 - \mathcal{M}_{11}^2}. \quad (10)$$

Here, we have set h to be the 125 GeV scalar and denoted the mass of H as m_H , which can be larger as well as smaller than 125 GeV depending on the parameters of the scalar potential. Since the most stringent constraint on the parameter space of this model comes from the collider searches of the doubly charged Higgs, its branching ratios in different channels play a crucial role. Hence, we will treat the mass of the 5-plet state, 3-plet state, and 125 GeV scalar as our input parameter and will trade off three potential parameters in terms of them. Thus, the final set of input parameter for our study is $m_5, m_3, s_H, \lambda_2, \lambda_3, \lambda_4, M_2$.

In this model, the 5-plet states couple to vector boson pairs as opposed to the 3-plet states, which only couple to fermions. Let us in this context define the quantities, ζ_W , ζ_Z , and ζ_f , which reflect the strengths of the W , Z and fermionic coupling, of H normalized to the similar couplings of the SM Higgs, respectively [24],

$$\zeta_Z = \frac{g_{HZZ}^{GM}}{g_{hZZ}^{SM}} = \frac{\sqrt{2}}{v} \sum_k \beta_{ki} v_k^c Y_k^2 \quad (11)$$

$$\zeta_W = \frac{g_{HWW}^{GM}}{g_{hWW}^{SM}} = \frac{\sqrt{2}}{v} \sum_k \beta_{ki} \left(v_k^c Y_k + v_k^r \frac{1}{4} \sqrt{n_k^2 - 1} \right) \quad (12)$$

$$\zeta_f = \frac{g_{Hff}^{GM}}{g_{hff}^{SM}} = \beta_{12} v / v_\phi, \quad (13)$$

where β is the matrix that rotates (h, H, H_5^0) to (ϕ^r, χ^r, ξ^r) and summation is over all the scalar multiplets participating in EWSB. In Eqs. (11) and (12), $i = 2$. $n_k^r = 3$ for the single real triplet ξ , while v_k^c and v_k^r are the vevs of the complex and real multiplets, respectively. As long as the custodial symmetry is preserved at both the potential and the vacuum level, $\zeta_W = \zeta_Z = \zeta_V = \sin \alpha \frac{v_\phi}{v} + \frac{8}{\sqrt{3}} \cos \alpha \frac{v_\chi}{v}$,

and breaking of custodial symmetry will introduce a splitting between them. Also with custodial symmetry, $\beta_{12} = \sin \alpha$ and $\beta_{13} = 0$. Another remarkable feature of this model is the presence of the nonzero $H^\pm W^\mp Z$ coupling. With custodial symmetry intact, only H_5^\pm has this kind of coupling, and when the symmetry is broken, a nonzero $H_3^\pm W^\mp Z$ vertex strength starts to appear. For the custodial symmetric case, this coupling strength is a simple scaling to s_H by a factor of $\frac{2M_W^2}{Vc_W}$, where c_W is the cosine of the Weinberg angle. But when the custodial symmetry is broken, this coupling takes a complicated form. For this case, let us define two quantities,

$$\kappa_{H_5^\pm W^\mp Z} = \frac{g_{H_5^\pm W^\mp Z}^{NC}}{[g_{H_5^\pm W^\mp Z}^{CS}]_{s_H=1}} \quad (14)$$

$$\kappa_{H_3^\pm W^\mp Z} = \frac{g_{H_3^\pm W^\mp Z}^{NC}}{[g_{H_3^\pm W^\mp Z}^{CS}]_{s_H=1}}, \quad (15)$$

where $g_{H_5^\pm W^\mp Z}^{NC}$ and $g_{H_3^\pm W^\mp Z}^{NC}$ denote the $H_5^\pm W^\mp Z$ and $H_3^\pm W^\mp Z$ interaction vertex strengths for the $v_\chi \neq v_\xi$ case and $g_{H_5^\pm W^\mp Z}^{CS}$ denotes the $H_5^\pm W^\mp Z$ interaction vertex strength for the custodial symmetric case. The expressions of $g_{H_5^\pm W^\mp Z}$, following a general derivation given [24], are

$$g_{H_i^\pm W^\mp Z} = \frac{g^2}{\sqrt{2} \cos \theta_W} \Sigma_k \alpha_{ki} (f_k^c v_k^c + f_k^r v_k^r), \quad (16)$$

where α is the 3×3 matrix that diagonalizes the singly charged scalar mass matrix in the (ϕ^+, χ^+, ξ^+) basis, $f_k^c = \sqrt{n_k^c - 1}(\cos^2 \theta_W - Y_k)$, $f_k^r = \frac{1}{2} \sqrt{n_k^r - 1} \cos^2 \theta_W$. Here, f_k^c corresponds to $k = 1, 2$ comprising ϕ and χ , with $n_k^c = 2$ and 3 , respectively. Similarly, f_k^r corresponds to ξ with $k = 3$ and $n_k^r = 3$. In the situation where $v_\chi = v_\xi$, the $H^\pm W^\mp Z$ coupling is possible for H_5^\pm only, and then the expression in Eq. (16) reduces to

$$g_{H_5^\pm W^\mp Z} = \frac{-gm_W s_H}{\cos \theta_W}. \quad (17)$$

It should be noted that the assertion $v_\chi = v_\xi$, based on Eq. (1) and the invariance of the potential under the custodial $SU(2)$ can be exactly ensured at the tree level only. However, the kinetic energy terms explicitly break the custodial $SU(2)$ via $U(1)_Y$ interactions. This at higher orders violates the custodial symmetry of the potential, resulting $v_\chi \neq v_\xi$ (unless there is fine-tuning). It is therefore useful to also estimate the modifications to the constraints on the parameter space, when the real and complex triplet vevs are unequal. In particular, the various points itemized in the previous section need to be revisited for such a

situation. The higher-order modifications, however, lead to large contributions to mass parameters in the potential, which in general shift them to the upper limit of validity of the GM scenario. Therefore, in case the triplet sector is expected to have bearing on accessible phenomenology, the GM model will have to pass the baton to some overseeing scenario not too far above the TeV scale, which controls the divergent corrections [37–39]. This essentially brings in new interactions, symmetries, or degrees of freedom. Thus, it is difficult to compute the modified potential in terms of the GM parameters alone. Keeping this in mind, we study the constraints for $v_\chi \neq v_\xi$ in Sec. IV, using some illustrative scenarios introduced in a phenomenological manner.

III. CONSTRAINTS FOR $v_\chi = v_\xi$

We start by updating and extending the existing constraints on the parameter space of the GM scenario. Before stating explicitly where we have gone beyond the studies already performed in this direction [18,19], a few general comments are in order.

The limits obtained in most works including ours are in terms of the mass of the 5-plet of the custodial $SU(2)$ [18,19,40]. In particular, it is meaningful to find the allowed upper limits of the quantity s_H , which is a measure of the triplet vev relative to the effective vev v driving EWSB, for various values of the doubly charged scalar mass. Stronger bounds of this kind come from direct searches in the 5-plet sector rather than those in the 3-plet sector because the production rates for this sector at the LHC are suppressed by $\frac{8v^2}{v_\phi^2}$ relative to the SM Higgs. Now, members of the 3-plet decay in fermionic channels only, where decays into tau(s) is one's most favorable option in terms of cleanliness of the signal. With the production rate already suppressed, the final states containing taus offer rather poor statistics, so the limits cannot be significant.

As far as the 5-plet sector is concerned, the neutral or the singly charged member yields weaker limits on s_H than what one obtains for the doubly charged component. For H_5^{++} , on the other hand, there are in principle various decay channels like $W^\pm W^\pm$, $H_3^\pm W^\pm$, $H_3^\pm H_3^\pm$ as also $\ell^\pm \ell^\pm$ when $\Delta L = 2$ Yukawa couplings exist. Same-sign dileptons, wherever available out of such final states, make up for the generally existing s_H suppression by virtue of the relatively ‘‘clean’’ visible peaks. That is why it is more profitable to attempt setting limits on s_H against $m_{H_5^{\pm\pm}}$, keeping of course in view other considerations going beyond direct searches.

Among the channels listed above, $H_5^{++} \rightarrow \ell^+ \ell^+$ is undoubtedly the most spectacular signal, where one notices a peak in the invariant mass distribution of the same-sign dileptons [41]. However, given the potential contribution of this scenario to neutrino masses via the Type-2 seesaw mechanism, a significant branching ratio for $H_5^{++} \rightarrow \ell^+ \ell^+$ will require $v_\chi \leq 10^{-10}$ GeV [42,43]. This, however, is a

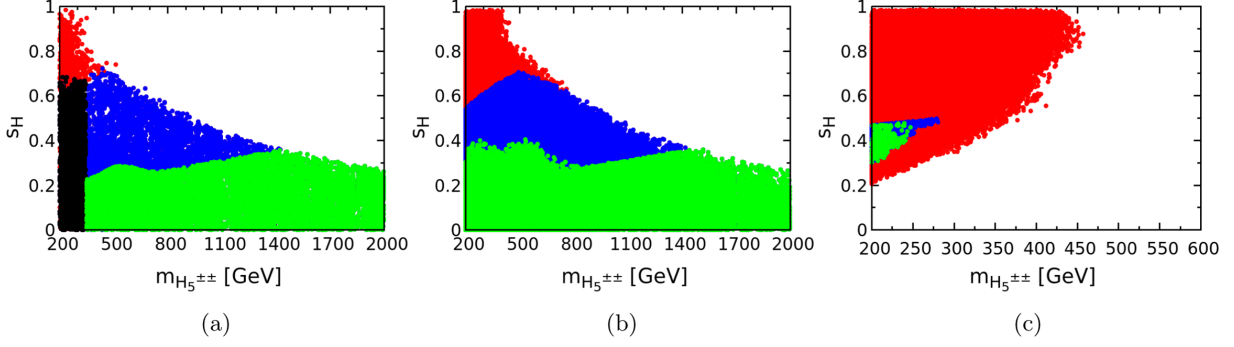


FIG. 1. Constraints on the $m_{H_5^{++}} - s_H$ plane. Figures 1(a), 1(b), and 1(c) correspond, respectively, to the situations of single, double, and triple-channel decay of H_5^{++} . Red, black, and blue regions are excluded by indirect constraints, DY search of H_5^{++} , and VBF search of H_5^{++} respectively. Green regions are allowed by all constraints.

situation far removed from those which are our main focus here, namely, the viability of substantial role of triplets in EWSB. We therefore keep the $\ell^\pm\ell^\pm$ decay channel out of our consideration.

Among the three remaining channels mentioned above, $H_3^\pm W^\pm$ and $H_3^\pm H_3^\pm$ will have the 3-plet charged scalars mostly decaying into quarks, in which case the leptons, even if produced, are likely to be degraded in cascades. Their detection is therefore relatively inefficient, and no analysis exists on these two channels so far. They, however, may serve to suppress the branching ratio into $W^\pm W^\pm$, thereby weakening the limits and allowing higher values of s_H for a given m_5 , at least from direct search at the LHC. We therefore extend the existing analyses for not only the single decay channel $H_5^{++} \rightarrow W^\pm W^\pm$ but also with either one or two of the additional channels mentioned above. In addition, the following constraints are taken into account:

- (i) Indirect constraints [44], primarily from the experimental bounds on the rates for $b \rightarrow s\gamma$ [45] and $B_s \rightarrow \mu^+\mu^-$ [46] and also from oblique electroweak parameters (of which the limit from T , or equivalently the ρ parameter, is explicitly used at every step).
- (ii) Theoretical constraints such as perturbative unitarity, vacuum stability, and the requirement that the custodial symmetry preserving vacuum corresponds to the global minimum of the potential [47,48].
- (iii) Whatever constraints come within the scope of the package GMCALC [49] have been made use of. We have updated them, using our own code for VBF with 137 fb^{-1} and DY with 139 fb^{-1} . The consistency of the code developed by us has been checked against GMCALC in the appropriate limits.
- (iv) All other constraints from the searches for additional neutral searches obtained using the code HIGGS-BOUNDS-5 [50].
- (v) The requirement that the signal strength of the 125 GeV scalar in all channels is consistent with LHC data. For this, the code HIGGSIGNALS-2 [51] has been made use of.

In obtaining the scatter plots presented in Figs. 1–3, the quantities whose specific values have entered as independent variables are m_5 , m_3 , and s_H , all other parameters in the GM scalar potential being subjected to an *unbiased scan*, subject to the requirements of unitarity, vacuum stability, and the demand that the EWSB vacuum corresponds to global minimum of the potential. The mass parameter (m_5) corresponding to the custodial 5-plet has been varied in the range 200 GeV–2 TeV, subject to the constraints mentioned above. The 3-plet mass m_3 is also subjected similar constraints, with its maximum allowed values being set according to the different kinematic situations described in the next paragraph. In cases where the 3-plet is never produced in decays of the doubly charged scalar H_5^{++} , the scan has been extended up to $m_3 = 5 \text{ TeV}$. The quantity s_H has been scanned over the entire allowed range of positive values, namely, $[0, 1]$.

Figure 1 contains the updated constraints obtained through our analysis, while the coupling strength modifications over the allowed region are shown in Fig. 2, taking as illustration the custodial-singlet neutral state H . Figures 1(a)–1(c) correspond, respectively, to single-channel ($H_5^{++} \rightarrow W^+W^+$), double-channel ($H_5^{++} \rightarrow W^+W^+, H_3^+W^+$), and triple-channel ($H_5^{++} \rightarrow W^+W^+, H_3^+W^+, H_3^+H_3^+$) decays allowed for the doubly charged state. In Fig. 2, the left, central, and right columns fall in these three kinematic categories.

Figure 3 illustrates the modified branching ratios of the CP -even, custodial-singlet scalar H in the $Z\gamma$ and $\gamma\gamma$ channels. This may be compared with the corresponding branching ratios of the SM Higgs boson.

While the three sets of figures and their corresponding captions are self-explanatory, the following features exhibited by them need to be commented upon:

- (i) The additional integrated luminosity accumulated up to 137 fb^{-1} puts additional constraints on s_H via the VBF channel. Thus, the upper limit in the case of single-channel H_5^{++} decay becomes more stringent compared to that found in Ref. [19], especially for masses exceeding 500 GeV.

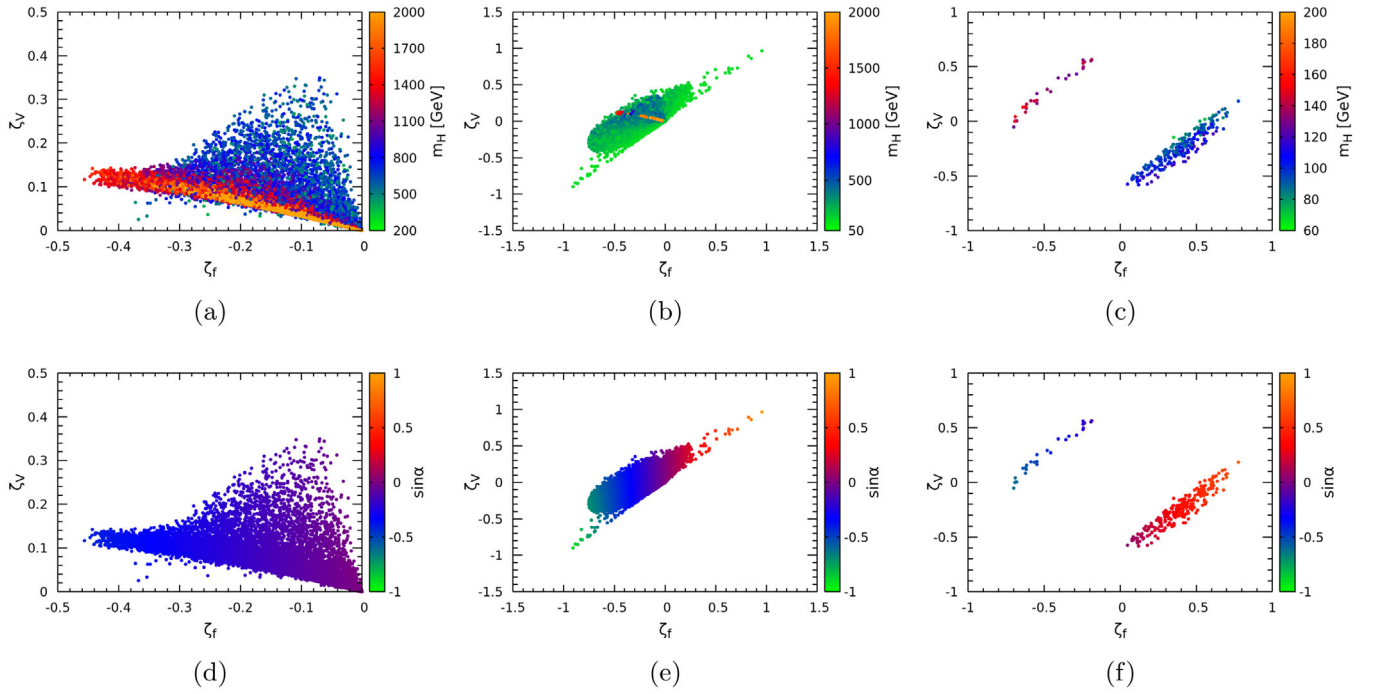


FIG. 2. Correlated modification factors in coupling strengths for the neutral scalar H to weak boson pairs and fermion pairs with respect to the corresponding couplings of the SM Higgs for single-channel (a and d), double-channel (b and e), and triple-channel (c and f) decays of H_3^{++} . The color axis in (a), (b), and (c) corresponds to m_H , the mass of H , while in (d), (e), and (f), it corresponds to $\sin \alpha$, the $SU(2)_L$ doublet content of H .

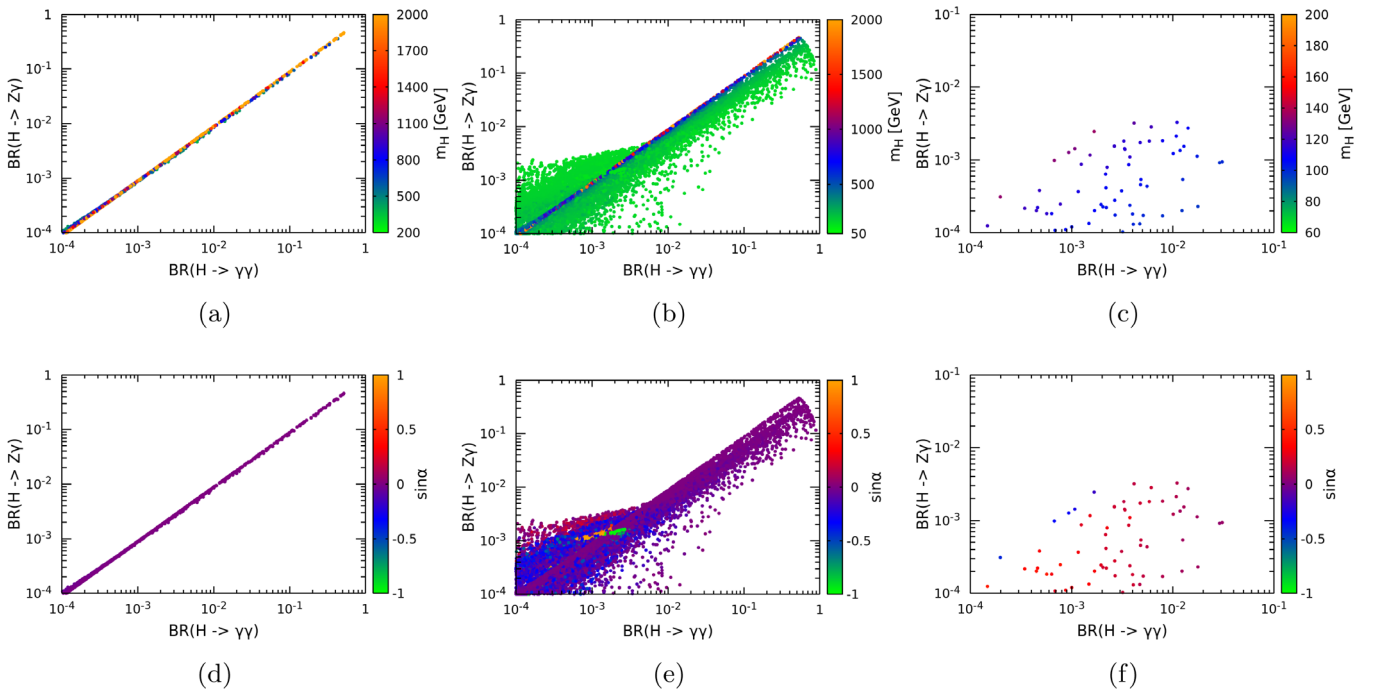


FIG. 3. Correlated branching ratios for $H \rightarrow Z\gamma$ and $H \rightarrow \gamma\gamma$ for single- (a and d), double- (b and e), and triple-channel (c and f) decay of H_3^{++} . The color axis in (a), (b), and (c) correspond to m_H , the mass of H , while in (d), (e), and (f), it correspond to $\sin \alpha$, the $SU(2)_L$ doublet content of H .

- (ii) When the decay channel into $H_3^+ W^+$ opens up, the limits from VBF are relatively relaxed and can go up to $s_H \approx 0.4$ at 500 GeV, where the earlier limit is 0.28 [18,19].
- (iii) All three aforementioned decays open up for a rather limited region of the parameter space, which ends around $m_5 \approx 300$ GeV. This is because it is not possible beyond this mass to satisfy Eqs. (5) and (6) simultaneously, without creating an unacceptable tension between the potential minimization conditions and unitarity limits on the quartic couplings. However, as expected, higher values of s_H (up to about 0.44) get allowed within this range, as compared to both the single- and double-channel decay situations. Looking at it from another angle, the higher m_5 is, the more difficult it is to keep m_3 small enough for the above channel to open up.
- (iv) The allowed values of s_H goes down significantly for large m_5 . The reason for this is understood if one looks at Eqs. (3) and (5). A high mass for H_5^{++} is largely governed by M_1 . Unless the triplet vev v_χ (and therefore s_H) is small, large M_1 would enhance some of the quartic couplings, ending up in unitarity violation.
- (v) The Drell-Yan channel has also been taken into account for 139 fb^{-1} of integrated luminosity. For the single-channel case, this practically excludes the mass range 200–300 GeV for the doubly charged scalar.² The DY limits, however, are progressively weaker for the two- and three-channel cases, as the sensitivity goes down proportionally with the squared branching ratio into $W^+ W^+$.
- (vi) The code HIGGSBOUNDS-5 has been used to constrain the particle spectrum from neutral Higgs searches at the LHC as well as LEP. However, the limits thus obtained are weaker than those from VBF [16,54]. As for the constraints from HIGGSIGNALS-2, the allowed regions shown the Figs. 1(a) and 1(b) are consistent at 95% C.L. However, the low H_3^+ masses relevant to the three-channel case tend to create more tension with the measurements of the diphoton signal strength for the 125 GeV scalar. This explains, for instance, the paucity of allowed points in Fig. 2(c), in which 95% C.L. consistency with HiggsSignals results are explicitly demanded.
- (vii) Figure 2 shows the modifications of the couplings for the custodial-singlet neutral scalar H to fermion and gauge boson pairs, as compared to those for the SM Higgs boson. As is particularly evident in Figs. 2(d)–2(f), the modifications are indicative of the $SU(2)$ doublet content of this state and can have bearings on its detectability at colliders. It should be noted that this content can be distinctly higher in the double- and triple-channel cases, although the regions of the parameter space answering to such enhancement are rather small.
- (viii) As seen from Fig. 3, it is possible for both the $\gamma\gamma$ and $Z\gamma$ branching ratios of the custodial singlet H to be considerably larger than those of the SM Higgs boson. This is because of some interesting features of this scenario. First, the tree-level decays of H into fermions get suppressed, since such decays are driven by its doublet component alone. Similarly, the role of the triplets in decays into gauge boson pairs is suppressed by the triplet vev. Such reduction in the share of tree-level decays results in the enhancement of the loop-induced $\gamma\gamma$ and $Z\gamma$ branching ratios. Second, while the fermion loops involve only the doublet component, the triplet part, too, drives the gauge boson loop amplitude. As a consequence, for a relatively small fraction of points used in the scan, the destructive interference between the fermion and gauge boson loops becomes constructive. More importantly, the charged scalar loop contribution has a rather strong constructive interference with the fermion loops.
- (ix) As has been mentioned already, a striking feature of this scenario (and in general of any theory containing scalar multiplets with nonzero vev possessing different values of Y) is tree-level interaction involving a charged Higgs, a W boson, and a Z boson [6,24], which can have interesting implications in triplet scalar phenomenology. For $v_\chi = v_\xi$, the strength of this interaction is proportional to s_H . This proportionality does not hold when the complex and real triplet vevs are unequal, as given in Sec. II. The numerical constraints on the $H^+ W^- Z$ couplings in such cases are explicitly obtained in the next section.

IV. CONSTRAINTS FOR $v_\chi \neq v_\xi$

So far, we have discussed the constraints corresponding to $v_\chi = v_\xi$, which is a direct consequence of the custodial $SU(2)$ symmetry of the scalar potential. Although this symmetry has been shown to be preserved in scalar loop corrections [12], it is in general liable to be broken on inclusion of gauge couplings. This is because hypercharge interactions in the scalar covariant derivatives break the custodial $SU(2)$. We have studied the constraints on model

²For masses below 200 GeV, the DY limits [52,53] are weaker compared to those from VBF.

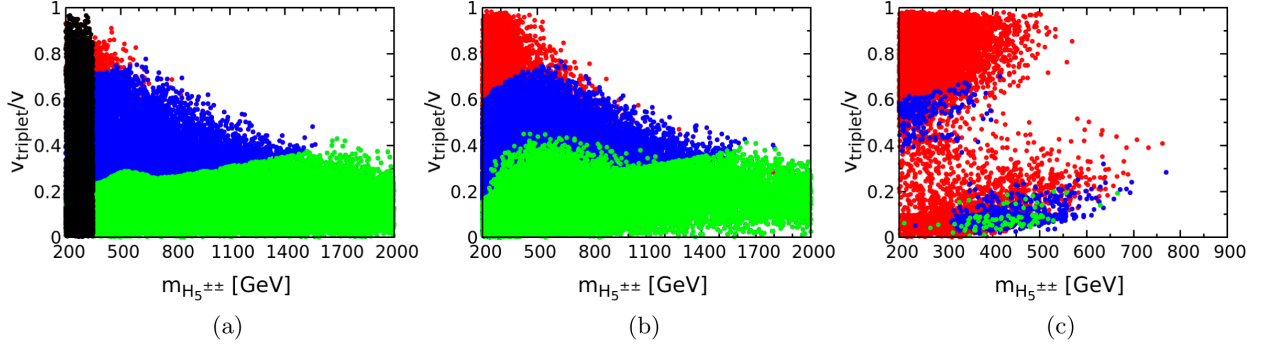


FIG. 4. Constraints on the $m_{H_5^{\pm\pm}} - \left(\frac{v_{\text{triplet}}}{v}\right)$ plane for $v_\chi \neq v_\xi$. Figures 1(a), 1(b), and 1(c) correspond, respectively, to the situation of single-, double-, and triple-channel decay of H_5^{++} . Red, black, and blue regions are excluded by indirect constraints, DY search of H_5^{++} , and VBF search of H_5^{++} , respectively. Green regions are allowed by all constraints.

parameters and associated issues, in such a situation as well, as reported below.

The higher-order corrections mentioned above entail quadratically divergent terms [22]. If the triplet scalar mass terms in the GM scenario have to be around the TeV scale or less (which is the situation where the GM model is phenomenologically significant), then some additional inputs have to come in the form of a cutoff for the GM theory. This has prompted us to use some phenomenological inputs for $v_\chi \neq v_\xi$.

Our investigation pertains to cases where the theoretical limits (which in principle requires some knowledge of the overseeing theory controlling the divergent contributions) are not substantially different from those in the corresponding cases with $v_\xi = v_\chi$. A similar consideration applies to indirect constraints.³

We have thus treated v_χ and v_ξ as phenomenological inputs, with their difference not exceeding 30% in our randomly generated points. In a similar fashion, the parameters in all scalar mass-squared matrices have been subjected to random variation, without differing by more than 30% with respect to values yielding $v_\chi = v_\xi$. After diagonalizing the mass matrices, the couplings of the physical scalar states have been calculated using FEYNRULES [55]. It has been checked that replacing 30% by 50% in the random number generation criteria does not make any qualitative change in the final results presented below. Apart from these, the general guidelines followed in obtaining the scatter plots (Figs. 4–9) are similar to those used in the previous section.

The quantity s_H , which in the previous cases uniquely parametrized the triplet contribution to the “effective vev” breaking the electroweak symmetry, is not similarly applicable when $v_\chi \neq v_\xi$. We instead make use of the quantity

³It should be remembered that the inequality of the two kinds of triplet vevs results in $H_3^+ W^- Z$ interactions, too, which alters the limits from precision electroweak observables. Similarly, H_5^\pm now develops small fermion couplings.

$$\frac{v_{\text{triplet}}}{v} = \frac{\sqrt{4(v_\chi^2 + v_\xi^2)}}{v}, \quad (18)$$

where $v = \sqrt{v_\Phi^2 + 4(v_\chi^2 + v_\xi^2)}$ is the effective vev. Since the custodial symmetry is broken, the physical states no longer constitute the irreducible representations under the custodial $SU(2)$ group. Hence, all the H_5 states will now have nonzero component coming from the $SU(2)_L$ doublet Φ .⁴ Similar effects will be seen in states belonging to the other representations of the custodial $SU(2)$. The contribution of $\phi^{0'}$ in H after this is denoted by β_{12} .

Figure 4 shows the allowed regions in the space spanned by $m_{H_5^{\pm\pm}}$ and $\frac{v_{\text{triplet}}}{v}$, with Figs. 4(a)–4(c) corresponding to the single-, double-, and triple-channel decays of the doubly charged scalar. The different coupling strength modification factors of the custodial singlet H are presented in Figs. 4–7. It is to be noted in this context that the WW and ZZ coupling strengths for the state H are liable to differ for $v_\chi \neq v_\xi$, a feature that affects the modification of interaction strengths in comparison with those for the SM Higgs. The allowed branching ratios for $H \rightarrow \gamma\gamma, Z\gamma$ are shown in Fig. 8. Figure 9 demonstrates the allowed points in the space spanned by the values of the $\kappa_{H_3^+ W^- Z}$ and $\kappa_{H_5^+ W^- Z}$, following the expressions given in Sec. II.

The salient points noticed in Figs. 4–9 are as follows:

- (i) The maximum value of $\frac{v_{\text{triplet}}}{v}$ remains comparable to that of s_H in the custodial symmetry preserving case, when one considers situations allowing single- and double-channel decays of the doubly charged Higgs.

⁴The mixing between the custodial 3-plet and the 5-plet will in principle also allow $H_5^{++} \rightarrow H_5^+ W^+$, resulting in a new two-channel ($H_5^{++} \rightarrow W^+ W^+$, $H_5^{++} \rightarrow H_5^+ W^+$), three-channel ($H_5^{++} \rightarrow W^+ W^+$, $H_5^{++} \rightarrow H_5^+ W^+$, $H_5^{++} \rightarrow H_3^+ W^+$), and even four-channel ($H_5^{++} \rightarrow W^+ W^+$, $H_5^{++} \rightarrow H_5^+ W^+$, $H_5^{++} \rightarrow H_3^+ W^+$, $H_5^{++} \rightarrow H_3^+ H_3^+$) decay modes. However, the unitarity of such mixing implies that the constraints will not be strengthened further.

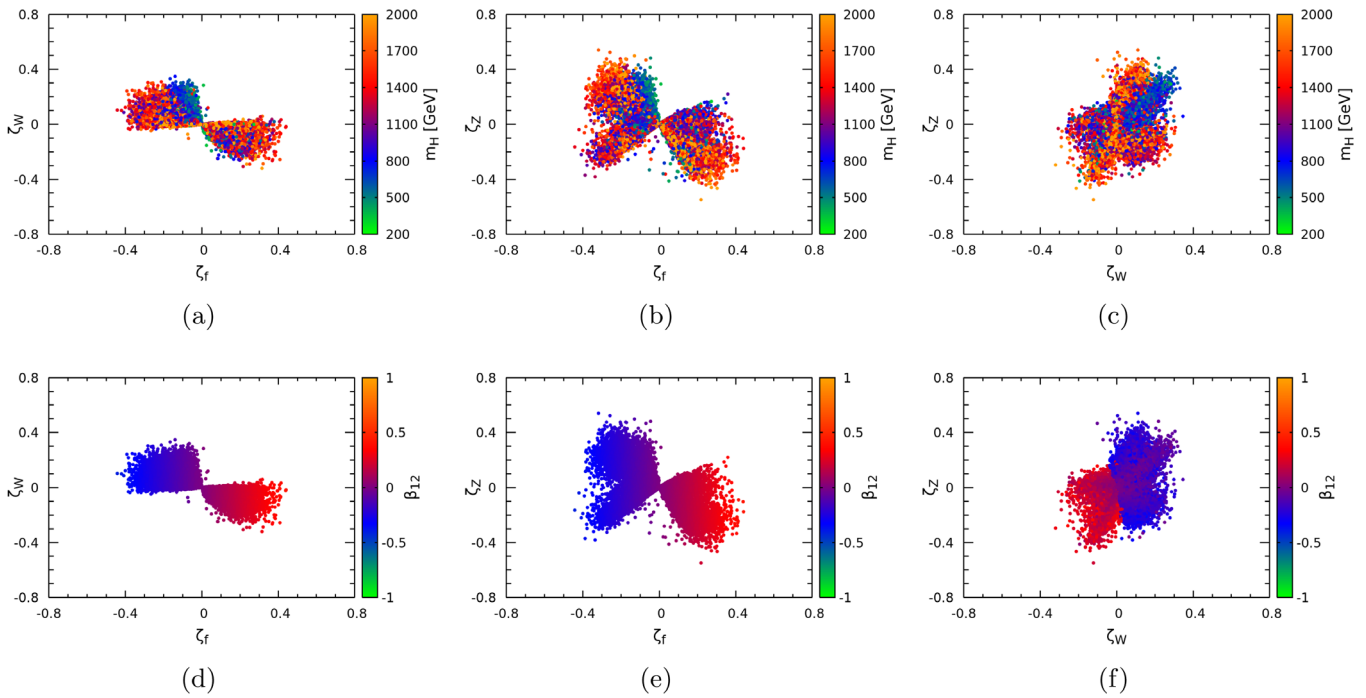


FIG. 5. Correlated modification factors in coupling strengths for the neutral scalar H to W , Z , and fermion pairs with respect to the corresponding couplings of the SM Higgs for single-channel decay of H_5^{++} for $v_\chi \neq v_\xi$. The color axis in (a), (b), and (c) corresponds to m_H , the mass of H, while in (d), (e), and (f), it corresponds to β_{12} , the $SU(2)_L$ doublet content of H.

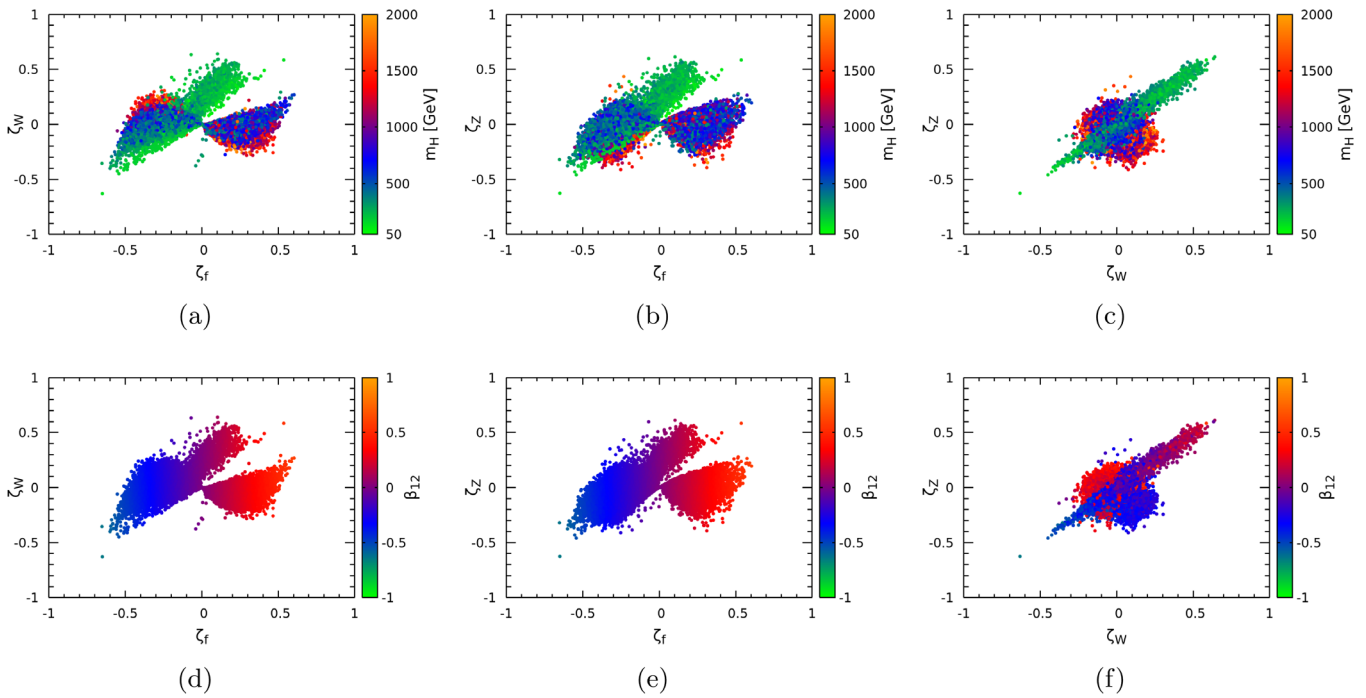


FIG. 6. Correlated modification factors in coupling strengths for the neutral scalar H to W , Z , and fermion pairs with respect to the corresponding couplings of the SM Higgs for double-channel decay of H_5^{++} for $v_\chi \neq v_\xi$. The color axis in (a), (b), and (c) corresponds to m_H , the mass of H, while in (d), (e), and (f), it corresponds to β_{12} , the $SU(2)_L$ doublet content of H.

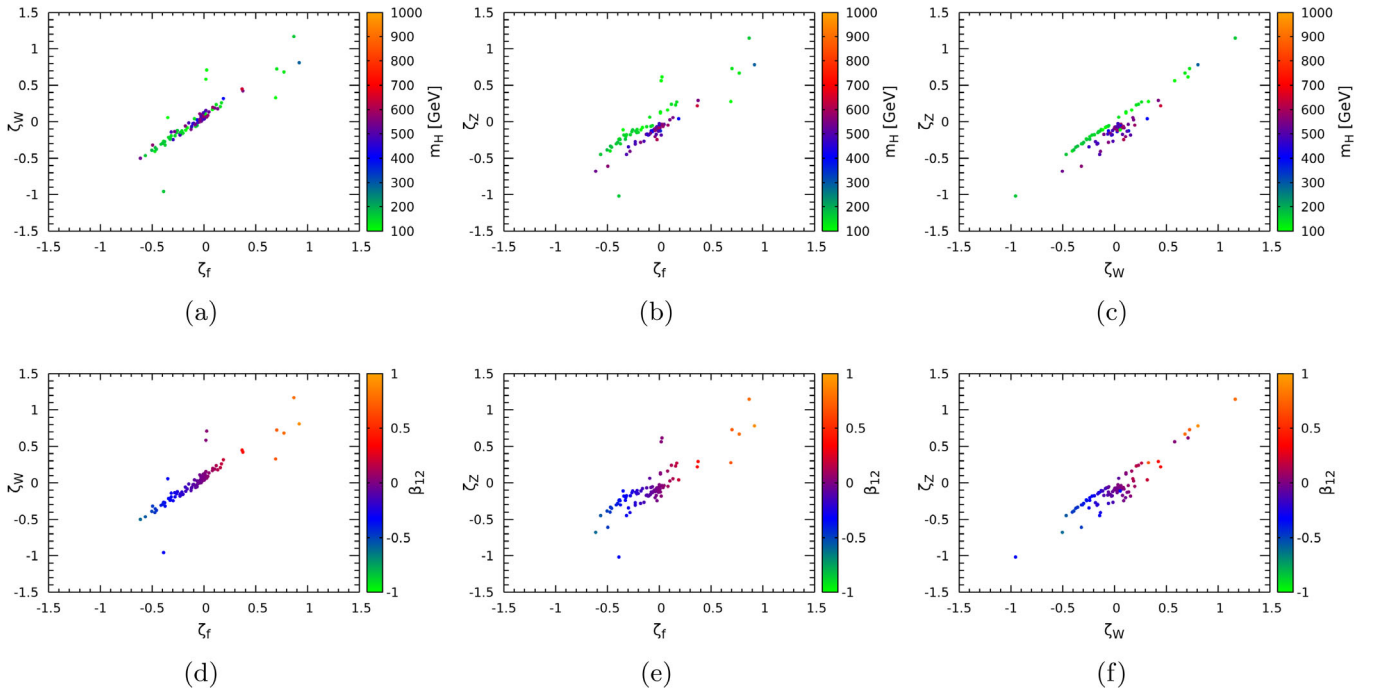


FIG. 7. Correlated modification factors in coupling strengths for the neutral scalar H to W , Z , and fermion pairs with respect to the corresponding couplings of the SM Higgs for triple-channel decay of H_S^{++} for $v_\chi \neq v_\xi$. The color axis in (a), (b), and (c) corresponds to m_H , the mass of H , while in (d), (e), and (f), it corresponds to β_{12} , the $SU(2)_L$ doublet content of H .

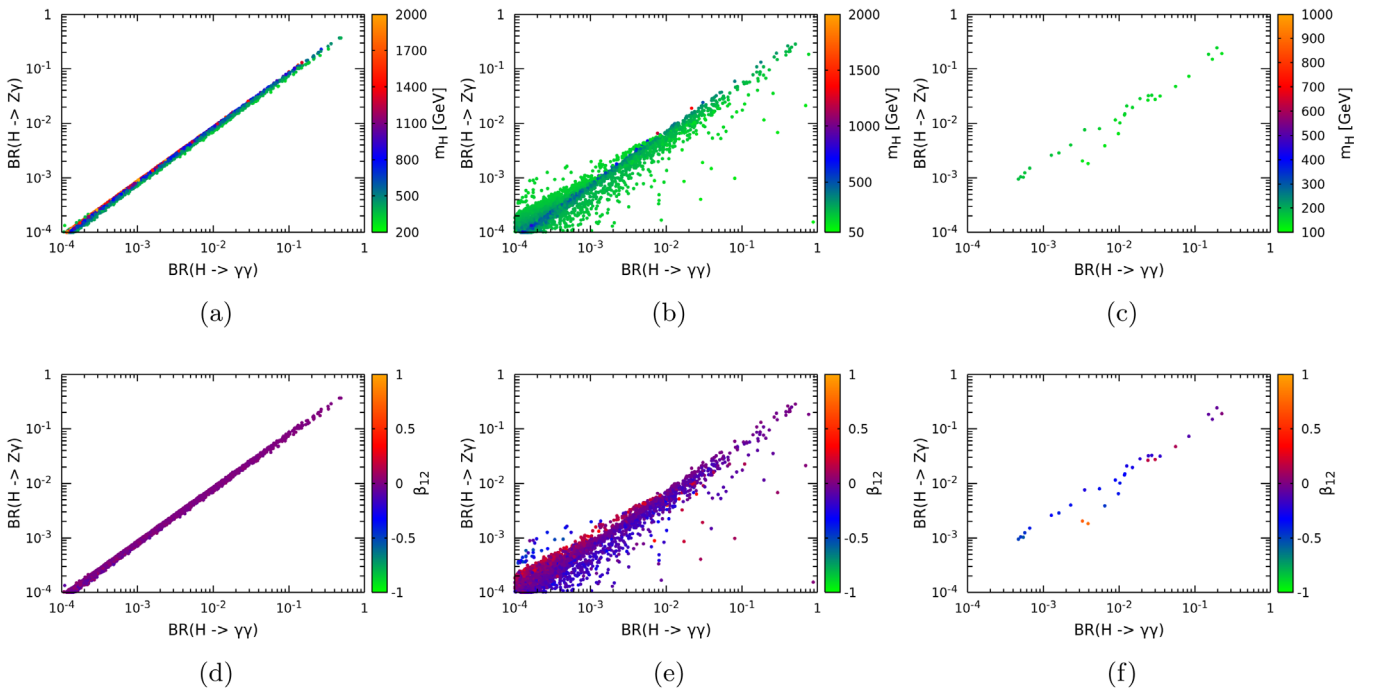


FIG. 8. Correlated branching ratios for $H \rightarrow Z\gamma$ and $H \rightarrow \gamma\gamma$ for single- (a and d), double- (b and e), and triple-channel (c and f) decay of H_S^{++} for $v_\chi \neq v_\xi$. The color axis in (a), (b), and (c) corresponds to m_H , the mass of H , while in (d), (e), and (f), it corresponds to β_{12} , the $SU(2)_L$ doublet content of H .

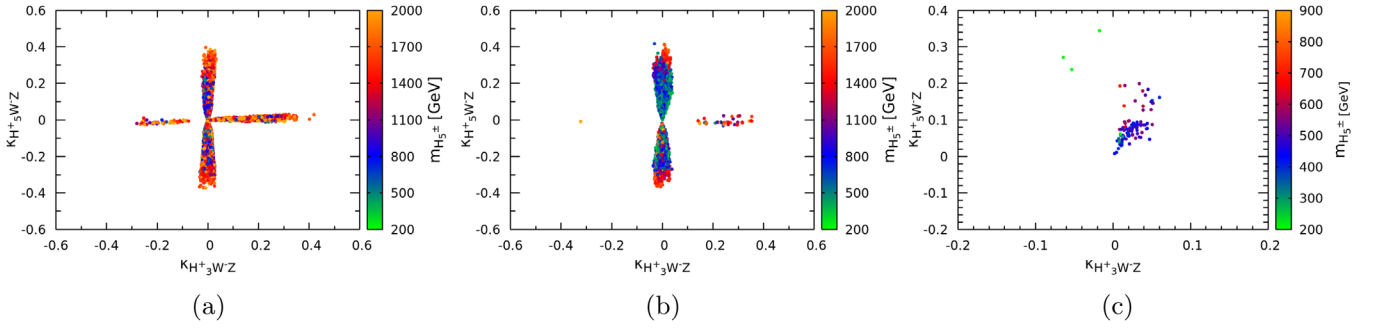


FIG. 9. The correlated vertex strength modification factors of $H_5^+ W^- Z$ and $H_3^+ W^- Z$ for $v_\chi \neq v_\xi$ with respect to the corresponding $H_5^+ W^- Z$ coupling strength in custodial symmetric case, as in Eq. (17) with $s_H = 1$. The color axis represents $m_{H_5^\pm}$, the mass of the singly charged scalar, which corresponds to H_5^\pm in custodial symmetric limit. Again, (a), (b), and (c) correspond, respectively, to single-, double-, and triple-channel decays of H_5^{++} .

For three allowed channels, however, the constraints are relatively relaxed here, as the allowed inequality of the real and complex triplet vevs opens up some additional phase space, allowing $H_5^{++} \rightarrow H_3^+ H_3^+$ and thus eating into the branching ratio for $H_5^{++} \rightarrow W^+ W^+$, the primary search channel.

- (ii) H , the custodial singlet neutral scalar, can now have a larger number of allowed points with substantial doublet content, especially for cases with double- and triple-channel decays allowed, as seen from Figs. 5–7.
- (iii) As compared to the case with exact custodial symmetry, one can have larger mass splitting allowed between two custodial multiplets. It is thus possible to have allowed regions in the parameter space with the state H as high as a TeV, with the erstwhile 3- and 5-plet state lying as low as 500 GeV.
- (iv) Here, too, there are allowed regions in all three cases with enhanced branching ratios in the $\gamma\gamma$ and $Z\gamma$ channels for H decay. In general, for the parameter points where such enhancement occurs, the deciding factor turns out to be not only the vev split but also their absolute values, a fact that may not be visible in the scatter plots.
- (v) Because of the added freedom of differencing v_χ and v_ξ , the maximum permissible strength of the $H_5^+ W^- Z$ interaction can be stronger than that with $v_\chi = v_\xi$ over a non-negligible region of the parameter space. However, such interaction is found to be appreciably enhanced with respect to the case with $v_\chi = v_\xi$, when H_5^{++} exclusively decays to $W^+ W^+$, that is to say, in the single-channel case. This effect is less pronounced for the two- and three-channel cases where the limit is already relaxed for $v_\chi = v_\xi$.
- (vi) In practically all cases from Fig. 4 onward, the allowed parameter regions answering to three decay channels for H_5^{++} are rather restricted, largely due to the interconnected nature of parameters and the proliferation of conditions to satisfy. For the same

reason, the “allowed” or “disallowed” label of any point in a plot may get altered upon minute variation in parameter values. For example, such a status may be effected s_H altered in the second/third place after decimal. The broadly allowed regions are nonetheless represented faithfully.

- (vii) The possibility of mixture of the 5- and 3-plets allows tree-level $H_3^+ W^- Z$ interaction in this case. Such coupling is less abundant for the triple-channel H_5^{++} decay, since this mass hierarchy allows very few points which simultaneously pass through the checks imposed by HiggsBounds and HiggsSignals.

V. SUMMARY AND CONCLUSION

We have made an extensive analysis of the constraints on the parameter space of the GM scenario, based on existing data. These includes collider data (including VBF/Drell-Yan data at the LHC with integrated luminosity of $137/139 \text{ fb}^{-1}$), those on the SM-like 125 GeV scalar, indirect limits including those from rare heavy flavor decays, and also all theoretical guidelines such as vacuum stability and unitarity. Searches for the doubly charged scalar constitute the most spectacular way of probing such a scenario. We have gone beyond the usually adopted idea that the $W^+ W^+$ decay channel is the only significant one when it comes to situations with substantial triplet contributions to the weak gauge boson masses. Thus, we have carried detailed scans of the parameter space where the $W^+ H_3^+$ and $H_3^+ H_3^+$ decay modes also open up, thus eating into the branching ratio share of the $W^+ W^+$ mode.

It is found that, with all possibilities and constraints included, the upper limit on the value of s_H , a measure of the triplet contribution to the W and Z masses, goes up to about 0.4 with mass around 500 GeV, in contrast to studies based on earlier data where similar values are attainable for masses close to a TeV only, and with constraints coming from data with lower luminosity. We also note that the constraints from unitarity tend to suppress the maximum

value of s_H for large (≥ 1.5 TeV) $m_{H_5^{\pm\pm}}$, thanks to the relations among physical masses and quartic couplings. The H^+W^-Z couplings correspondingly have the scope of enhancement when two- and three-channel decays of the doubly charged scalar are allowed. We also note that, in such situations, the $\gamma\gamma$ and $Z\gamma$ branching ratios for the custodial singlet scalar H can sometimes be much higher than that of the SM-like scalar state.

While the above conclusions apply to the case with the custodial SU(2) symmetry intact, we extend our study to situations where the real and complex triplets have unequal vev's. In a phenomenological approach to parameter scans, we have demonstrated that a larger number of parameter

points can become allowed, subject to all constraints, and the features outlined above are more widely visible. In addition, the charged scalar H_3^+ , too, has W^-Z interaction here. Thus, the GM scenario still admits of interesting phenomenology, subject to the various constraints that tend to tie it up.

ACKNOWLEDGMENTS

The authors thank Utpal Sarkar, Tousik Samui, and Ritesh K Singh for helpful discussion. The work of R. G. has been supported by a fellowship awarded by University Grants Commission, India.

-
- [1] J. Tao (CMS Collaboration), *Nucl. Part. Phys. Proc.* **300**, 53 (2018); G. Aad *et al.* (ATLAS Collaboration), *J. High Energy Phys.* **08** (2022) 175; G. Aad *et al.* (ATLAS Collaboration), *Eur. Phys. J. C* **82**, 622 (2022); ATLAS Collaboration, [arXiv:2207.00348](https://arxiv.org/abs/2207.00348).
 - [2] H. S. Goh, R. N. Mohapatra, and S. Nasri, *Phys. Rev. D* **70**, 075022 (2004).
 - [3] B. Dutta, Y. Mimura, and R. N. Mohapatra, *Phys. Rev. D* **80**, 095021 (2009).
 - [4] G. Senjanovic and R. N. Mohapatra, *Phys. Rev. D* **12**, 1502 (1975).
 - [5] N. G. Deshpande, J. F. Gunion, B. Kayser, and F. Olness, *Phys. Rev. D* **44**, 837 (1991).
 - [6] J. F. Gunion, H. E. Haber, G. L. Kane, and S. Dawson, *Front. Phys.* **80**, 1 (2000).
 - [7] A. Maiezza, G. Senjanovic, and J. C. Vasquez, *Phys. Rev. D* **95**, 095004 (2017).
 - [8] P. H. Gu, H. Zhang, and S. Zhou, *Phys. Rev. D* **74**, 076002 (2006).
 - [9] A. Melfo, M. Nemevsek, F. Nesti, G. Senjanovic, and Y. Zhang, *Phys. Rev. D* **85**, 055018 (2012).
 - [10] M. E. Peskin and T. Takeuchi, *Phys. Rev. D* **46**, 381 (1992).
 - [11] H. Georgi and M. Machacek, *Nucl. Phys.* **B262**, 463 (1985).
 - [12] M. S. Chanowitz and M. Golden, *Phys. Lett.* **165B**, 105 (1985).
 - [13] H. Georgi and D. B. Kaplan, *Phys. Lett.* **145B**, 216 (1984).
 - [14] A. Kundu, P. Mondal, and P. B. Pal, *Phys. Rev. D* **105**, 115026 (2022).
 - [15] C. H. de Lima and H. E. Logan, *Phys. Rev. D* **106**, 115020 (2022).
 - [16] A. M. Sirunyan *et al.* (CMS Collaboration), *Eur. Phys. J. C* **81**, 723 (2021).
 - [17] M. Aaboud *et al.* (ATLAS Collaboration), *Eur. Phys. J. C* **78**, 199 (2018).
 - [18] A. Ismail, B. Keeshan, H. E. Logan, and Y. Wu, *Phys. Rev. D* **103**, 095010 (2021).
 - [19] A. Ismail, H. E. Logan, and Y. Wu, [arXiv:2003.02272](https://arxiv.org/abs/2003.02272).
 - [20] C. W. Chiang, S. Kanemura, and K. Yagyu, *Phys. Rev. D* **90**, 115025 (2014).
 - [21] J. F. Gunion, R. Vega, and J. Wudka, *Phys. Rev. D* **42**, 1673 (1990).
 - [22] J. F. Gunion, R. Vega, and J. Wudka, *Phys. Rev. D* **43**, 2322 (1991).
 - [23] C. W. Chiang and K. Yagyu, *J. High Energy Phys.* **01** (2013) 026.
 - [24] A. Kundu and B. Mukhopadhyaya, *Int. J. Mod. Phys. A* **11**, 5221 (1996).
 - [25] B. Mukhopadhyaya, *Phys. Lett. B* **252**, 123 (1990).
 - [26] R. Godbole, B. Mukhopadhyaya, and M. Nowakowski, *Phys. Lett. B* **352**, 388 (1995).
 - [27] D. K. Ghosh, R. M. Godbole, and B. Mukhopadhyaya, *Phys. Rev. D* **55**, 3150 (1997).
 - [28] G. Aad *et al.* (ATLAS Collaboration), *Phys. Rev. Lett.* **114**, 231801 (2015).
 - [29] A. Adhikary, N. Chakrabarty, I. Chakraborty, and J. Lahiri, *Eur. Phys. J. C* **81**, 554 (2021).
 - [30] A. Falkowski, S. Rychkov, and A. Urbano, *J. High Energy Phys.* **04** (2012) 073.
 - [31] C. W. Chiang, A. L. Kuo, and K. Yagyu, *Phys. Rev. D* **98**, 013008 (2018).
 - [32] C. Degrande, K. Hartling, and H. E. Logan, *Phys. Rev. D* **98**, 019901(E) (2018); **96**, 075013 (2017).
 - [33] C. W. Chiang, A. L. Kuo, and K. Yagyu, *Phys. Lett. B* **774**, 119 (2017).
 - [34] C. W. Chiang and T. Yamada, *Phys. Lett. B* **735**, 295 (2014).
 - [35] T. W. B. Kibble, *Phys. Rev.* **155**, 1554 (1967).
 - [36] P. W. Higgs, *Phys. Rev. Lett.* **13**, 508 (1964).
 - [37] L. Cort, M. Garcia, and M. Quiros, *Phys. Rev. D* **88**, 075010 (2013).
 - [38] M. G. Pepin, S. Gori, M. Quiros, R. Vega, R. V. Morales, and T. T. Yu, *Phys. Rev. D* **91**, 015016 (2015).
 - [39] R. Vega, R. V. Morales, and K. Xie, *J. High Energy Phys.* **03** (2018) 168.
 - [40] C. W. Chiang, A. L. Kuo, and T. Yamada, *J. High Energy Phys.* **01** (2016) 120.
 - [41] S. Ghosh, [arXiv:2205.03896](https://arxiv.org/abs/2205.03896).
 - [42] R. Primulando, J. Julio, and P. Uttayarat, *J. High Energy Phys.* **08** (2019) 024.

- [43] E. J. Chun, K. Y. Lee, and S. C. Park, *Phys. Lett. B* **566**, 142 (2003).
- [44] K. Hartling, K. Kumar, and H. E. Logan, *Phys. Rev. D* **91**, 015013 (2015).
- [45] J. P. Lees *et al.* (BABAR Collaboration), *Phys. Rev. D* **86**, 112008 (2012).
- [46] V. Khachatryan *et al.* (CMS and LHCb Collaborations), *Nature (London)* **522**, 68 (2015).
- [47] M. Aoki and S. Kanemura, *Phys. Rev. D* **89**, 059902(E) (2014); **77**, 095009 (2008).
- [48] K. Hartling, K. Kumar, and H. E. Logan, *Phys. Rev. D* **90**, 015007 (2014).
- [49] K. Hartling, K. Kumar, and H. E. Logan, [arXiv:1412.7387](https://arxiv.org/abs/1412.7387).
- [50] P. Bechtle, D. Dercks, S. Heinemeyer, T. Klingl, T. Stefaniak, G. Weiglein, and J. Wittbrodt, *Eur. Phys. J. C* **80**, 1211 (2020).
- [51] P. Bechtle, S. Heinemeyer, T. Klingl, T. Stefaniak, G. Weiglein, and J. Wittbrodt, *Eur. Phys. J. C* **81**, 145 (2021).
- [52] A. Delgado, M. G. Pepin, M. Quiros, J. Santiago, and R. V. Morales, *J. High Energy Phys.* **06** (2016) 042.
- [53] R. Vega, R. V. Morales, and K. Xie, *J. High Energy Phys.* **06** (2018) 137.
- [54] A. M. Sirunyan *et al.* (CMS Collaboration), *Phys. Rev. Lett.* **119**, 141802 (2017).
- [55] A. Alloul, N. D. Christensen, C. Degrande, C. Duhr, and B. Fuks, *Comput. Phys. Commun.* **185**, 2250 (2014).